fast DART
DATA, ANALYSIS, REVIEWS, TECHNIQUES E-JOURNAL

Original Research

Differential Regulation of UBE3A Expression Following Neuronal Activation

Melinda M Peters [1,2], Aurelie Joly-Amado [1,2], Kevin R Nash and [1,2], Edwin J Weeber [1,2]

[1]USF Health Byrd Alzheimer's Institute, Tampa, FL, 33613, USA
[2]Department of Molecular Pharmacology and Physiology, University of South Florida, Tampa, FL, USA

Article History
Submitted: September 18, 2025 Accepted: October 24, 2025 Published: November 1, 2025

Abstract

Angelman syndrome (AS) results from loss of the maternally inherited *UBE3A* allele, a neuronally imprinted gene essential for synaptic plasticity. While the maternal allele is active, the paternal copy is typically silenced, limiting therapeutic strategies. Here, we investigated activity-dependent regulation of maternal and paternal *Ube3a* using a YFP knock-in reporter that permits allele-specific protein quantification. In hippocampal slices, high-frequency stimulation and potassium depolarization triggered biphasic increases in UBE3A protein, with rapid early peaks and delayed secondary surges. Use of an in vivo, associative fear conditioning model revealed region-specific and allele-specific dynamics: hippocampal paternal *Ube3a* showed robust induction within 1–6 hours, maternal *Ube3a* exhibited sustained late upregulation, and parietal cortex expression from both alleles rose transiently within minutes. Prefrontal cortex responses were delayed, peaking at 6 hours. These results demonstrate that neuronal activity drives dynamic, allele-specific modulation of UBE3A across distinct cortical–hippocampal networks. Notably, paternal *Ube3a* can be transiently unsilenced following behavioral stimulation, revealing an untapped mechanism of regulation. This work highlights the potential to harness experience-dependent pathways to restore paternal UBE3A expression in AS, informing strategies for therapeutic reactivation.

Keywords: UBE3A, Angelman syndrome, paternal allele, maternal deletion, hippocampus, synaptic plasticity, neuronal activation, imprinting, Western blot, mouse model.

Introduction

Angelman syndrome (AS) is a rare neurodevelopmental disorder first described by Harry Angelman in 1965, characterized by severe intellectual disability, absent or minimal speech, ataxia, epilepsy, and a distinctive behavioral phenotype often described as a "happy demeanor" with frequent laughter and smiling. The estimated prevalence ranges from 1 in 10,000 to 1 in 20,000 live births (Buiting et al., 2016). Molecularly, AS is caused by loss of function of the maternally inherited *UBE3A* gene, which encodes the E6AP ubiquitin protein ligase, an E3 ligase involved in the ubiquitin–proteasome system that regulates protein turnover and synaptic function (Greer et al., 2010). In most neurons, UBE3A expression is subject to genomic imprinting, with the paternal allele silenced by a non-translating antisense transcript (UBE3A-ATS) (Meng et al., 2012; Meng et al., 2015; Hsiao et al., 2019). Thus, in neurons, only the maternal allele is active. The four primary molecular classes of AS are: 1. large deletions of the maternal 15q11q13 region (~70% of cases), which also encompass multiple other genes; 2. paternal uniparental disomy (UPD, ~2–5%), in which both

chromosome 15s are inherited from the father; 3. imprinting defects (~2–5%), which prevent activation of the maternal allele; and 4. intragenic mutations of UBE3A (~10%) (Keute et al., 2021). Rare cases involve chromosomal translocations or other structural variants (Fang et al., 1999).

Neuroanatomical studies in both human patients and animal models have revealed that AS pathology is not localized to a single brain region but reflects widespread network dysfunction (Gustin et al., 2010; Daily et al., 2012). MRI studies have noted reduced total brain volume, with particular involvement of the cerebellum, hippocampus, and certain cortical regions (Peters et al., 2011). Functional imaging and electrophysiological studies point to abnormalities in thalamocortical oscillations, hippocampal synaptic plasticity, and cerebellar motor circuits (Yoon et al., 2020; Du et al., 2023). Mouse models with maternal UBE3A deficiency display impaired long-term potentiation (LTP) in the hippocampus, altered excitatory/inhibitory balance in neocortex, and Purkinje cell dysfunction in the cerebellum, paralleling human motor and cognitive phenotypes (Weeber et al., 2003; Banko et al., 2011; Filonova et al., 2014; Pastuzyn and Shepherd, 2017). UBE3A protein is found throughout the CNS; however, protein levels vary considerably across brain regions. In wildtype mice, UBE3A is highly expressed in the hippocampus, particularly CA1 pyramidal neurons, cerebral cortex, cerebellar Purkinje cells, and various subcortical nuclei (Jiang et al., 1998; Yamasaki et al., 2003; Jones et al., 2016). Quantitative analyses have shown that the degree of UBE3A loss in AS models mirrors the neuron specific imprinting pattern, with virtually complete absence of UBE3A in most neurons, but preservation of expression in glial cells where the paternal allele remains active (Judson et al., 2014; Grier et al., 2015). Regional vulnerability may be linked to the functional roles of these neuronal populations. For example, loss of UBE3A in hippocampal and cortical neurons likely underlies cognitive and language impairments, while its absence in cerebellar Purkinje cells contributes to motor incoordination. Collectively, these findings frame AS as a systems level disorder of neural networks, in which a single gene defect disrupts synaptic homeostasis and plasticity across multiple brain regions. Understanding the spatial and cellular pattern of *Ube3a* expression, and its loss in AS, is critical for designing targeted therapeutic strategies, whether by restoring *Ube3a* expression, compensating for its absence, or modulating downstream pathways.

A particularly valuable tool for studying the spatial and temporal regulation of UBE3A expression is the *UBE3A-YFP* knock-in mouse model, in which a yellow fluorescent protein (YFP) tag is fused inframe to the Cterminus of the endogenous UBE3A protein (Dindot et al., 2008; Vihma et al., 2024). This genetic modification results in the production of a full length UBE3A-YFP fusion protein that retains the functional domains of the native E6AP ubiquitin ligase while acquiring the fluorescent tag for visualization *in situ*. The YFP moiety increases the molecular weight of UBE3A by approximately 27 kDa, producing a clear electrophoretic mobility shift on SDS-PAGE gels. This size difference allows the UBE3A-YFP fusion protein to be readily distinguished from the untagged endogenous form by basic Western blotting techniques, making it possible to differentiate maternal and paternal allele derived protein in tissues from heterozygous animals. Because the paternal *UBE3A* allele is silenced in neurons but remains active in most glial cells, Western blots from brain lysates of *UBE3A-YFP*/+ mice display two discrete bands corresponding to untagged maternal derived Ube3a and YFP tagged paternal derived Ube3a from glia, thereby providing a direct biochemical readout of allele specific expression. This system has been instrumental in quantifying the extent and cell type specificity of imprinting, validating reactivation strategies, and correlating restoration of paternal allele expression with functional rescue in preclinical studies (Vihma et al., 2024).

In the current study, the *Ube3a-YFP* knock-in mouse model is being leveraged to quantify allele-specific contributions to total Ube3a protein levels following neuronal activation induced by associative fear conditioning. This behavioral paradigm, which robustly engages hippocampal–amygdalar circuits and drives activity-dependent gene expression, provides a physiologically relevant context in which to examine dynamic regulation of the *Ube3a* locus. By analyzing brain regions harvested at defined time points after conditioning, Western blotting can distinguish the maternal-derived untagged Ube3a from the paternal-

derived YFP-tagged protein, thereby revealing potential changes in expression from either allele in response to neuronal activity. Such studies not only elucidate how experience-dependent plasticity influences Ube3a protein homeostasis but also illuminates the potential for activity-based or experience-dependent strategies to enhance paternal allele expression in therapeutic contexts for Angelman syndrome.

Materials and Methods

Animals

Angelman syndrome model mice lacking the maternally inherited *Ube3a* allele (*Ube3a^m−/p+*) on a C57BL/6J background were used (Jackson Laboratory, Bar Harbor, ME). Wild-type control mice (*Ube3a^m+/p+*) were generated by crossing wild-type males with *Ube3a^m−/p+* females. Tail or ear tissues were collected from pups before postnatal day 10 (P10) or after for genotyping. A two-primer PCR protocol was used, including P1 (common), P2 (wild-type reverse), and P3 (mutant) primers, under cycling conditions of 94 °C for 3 min followed by 30 cycles of 94 °C for 30 sec, 58.3 °C for 1 minute, and 72 °C for 1 minute. All experiments were conducted using adult (8–12 weeks old) mice, housed under a 12 hr light/dark cycle with ad libitum access to food and water. All procedures were performed in accordance with the National Institutes of Health Guide for the Care and Use of Laboratory Animals and were approved by the Institutional Animal Care and Use Committee (IACUC) of the University of South Florida.

Allele-Specific Expression via Ube3a-YFP Reporter

In the *Ube3a-YFP* knock-in model, the endogenous Ube3a is C-terminally tagged with YFP, increasing its molecular weight by ~27 kDa. This size shift enables differentiation between maternal and paternal Ube3a protein via Western blotting: the untagged maternal protein and YFP-tagged paternal, glial-expressed protein appear as distinct bands in heterozygous mice. This allows tracking of allele-specific expression dynamics following neuronal activation, such as fear conditioning—a method that reveals activity-dependent increases in both forms of Ube3a.

Hippocampal Slice Preparation

Acute hippocampal slices were prepared as described previously with minor modifications. Briefly, mice were deeply anesthetized with isoflurane and decapitated. Brains were rapidly removed and immersed in ice-cold, oxygenated (95% O_2/5% CO_2) cutting solution containing (in mM): 87 NaCl, 2.5 KCl, 25 $NaHCO_3$, 1.25 NaH_2PO_4, 75 sucrose, 25 glucose, 0.5 $CaCl_2$, and 7 $MgCl_2$. Transverse hippocampal slices (~350 μm) were cut using a VT1200S vibratome (Leica Microsystems) and transferred to an interface chamber containing artificial cerebrospinal fluid (aCSF; in mM: 124 NaCl, 3 KCl, 26 $NaHCO_3$, 1.25 NaH_2PO_4, 10 glucose, 2 $CaCl_2$, 1 $MgCl_2$) equilibrated with 95% O_2/5% CO_2. Slices were allowed to recover at 32 °C for 1 hr prior to experimentation.

Electrophysiological Stimulation

For synaptic activation experiments, slices were transferred to a submerged recording chamber perfused with oxygenated ACSF (2 mL/min, 30 °C). Field excitatory postsynaptic potentials (fEPSPs) were recorded from the CA1 *stratum radiatum* using glass microelectrodes (resistance 2–4 MΩ) filled with ACSF. The Schaffer collateral pathway was stimulated using a bipolar tungsten electrode. After establishing a stable baseline (10–15 min), long-term potentiation was induced using a high-frequency stimulation (HFS) protocol: 5 trains of 100 Hz stimulation (1 s duration per train, inter-train interval 20 s) at 60–70% of maximal fEPSP slope.

Potassium-Induced Depolarization

For depolarization experiments, slices were prepared identically to the electrophysiology cohort and were transferred to ACSF containing 50 mM KCl (NaCl reduced accordingly to maintain osmolarity) and incubated for the designated stimulation period before washout in normal ACSF.

Tissue Collection and Protein Extraction

At designated post-stimulation time points (0, 5, 15, 30, 60, and 120 min), slices were rapidly removed from the chamber, and the CA1 subfield was microdissected on an ice-cold surface. Tissue was flash-frozen in liquid nitrogen and stored at –80 °C until processing. Samples were homogenized in RIPA

buffer (50 mM Tris-HCl pH 7.4, 150 mM NaCl, 1% NP-40, 0.5% sodium deoxycholate, 0.1% SDS) supplemented with protease and phosphatase inhibitors (Thermo Fisher). Lysates were cleared by centrifugation (14,000 × g, 15 min, 4 °C), and total protein concentration was determined by BCA assay (Thermo Fisher).

Western Blotting for UBE3A Detection

Dissected brain regions (e.g., cortex, hippocampus, cerebellum) were rapidly harvested and frozen for protein analysis. Tissue samples were homogenized in RIPA buffer with protease inhibitors, and protein concentrations were determined via Bradford assay. Samples (1–3 μg/μL) were denatured at 60 °C for 10 min and separated on 10% SDS-PAGE gels. Proteins were transferred onto PVDF membranes and blocked overnight in 4% milk at 4 °C. Membranes were probed with primary antibodies including anti-UBE3A (Sigma E6855; 1:2000) and anti-actin (Millipore MAB1501; 1:50,000), followed by fluorescent secondary antibodies (LI-COR IRDye series; 1:10,000). Imaging was performed on a LI-COR Odyssey system, and quantitative analysis was conducted using commercial Odyssey software.

Associative Fear Conditioning

To evaluate associative learning, mice were subjected to a context-dependent fear conditioning protocol, which engages hippocampal and amygdalar circuits. Animals were placed in a conditioning chamber where they were exposed to paired presentations of a 90 dB tone (2 kHz, 30 seconds) that co-terminated with a mild foot shock (0.5 mA). Contextual memory was assessed by returning mice to the same chamber 24 hours later and measuring freezing behavior. In contrast, cued memory was evaluated by placing mice in a modified (novel) context with altered sensory cues and exposing them to the tone alone, recording freezing behavior accordingly.

Quantification and Statistical Analysis

Maternal and paternal alleles were analyzed separately using a one-way ANOVA, followed by Tukey's post hoc multiple comparisons test to assess differences between each time point and the "no shock" control. Normality was evaluated with the Shapiro–Wilk test and variance homogeneity was confirmed with Levene's test. Statistical significance was defined as $p < 0.05$. All data are reported as mean ± SEM, with exact p-values for significant comparisons provided in the figure or supplementary tables. All analyses were conducted in GraphPad Prism (v.10).

Both male and female mice were included. Mouse husbandry adhered to NIH and IACUC regulations.

Results

We investigated the acute regulation of Ube3a protein levels following neuronal activation in *ex vivo* hippocampal slices from wild-type mice. Field recordings were performed in CA1 slices using a standard high-frequency stimulation (HFS) protocol consisting of 5 trains of 100 Hz stimulation at Schaffer collateral synapses (Weeber et al., 2003) (Martinez and Derrick, 1996) (Selcher et al., 2002) (Malenka and Bear, 2004). Slice tissues were collected at 0, 5, 15, 30, 60, and 120 minutes post-stimulation, and CA1 regions were dissected for Western blot analysis. Ube3a levels (expressed as percentage relative to time 0 control) increased significantly to 22 ± 2.9% at 5 min and reached 35 ± 5.9% at 15 min. A modest reduction occurred by 30 min (12.2 ± 3.3%) before expression rebounded to 42 ± 12.2% at 60 min and peaked at 53.3 ± 8.9% by 120 min. These data indicate a biphasic Ube3a response with an initial surge, partial decline, and delayed secondary peak following synaptic activation.

In parallel, we attempted to mimic the effects of CA1 HFS-induced depolarization without using an electrical stimulation. Thus, we applied potassium-induced depolarization (using 50 mM KCl, standard for acute depolarization protocols) to hippocampal slices prepared identically to the electrophysiology experiments (Filonova et al., 2014) (Thomas et al., 1996). CA1 was similarly dissected at matched time points. Ube3a levels rose more rapidly and robustly under depolarization: 44.8 ± 7.6% at 5 min and 65.7 ± 18.3% at 15 min, followed by a decline to 7.9 ± 2.5% by 30 min. Similar to HFS, expression recovered at later time points, yielding 57 ± 14.6% at 60 min and a maximal increase of 78.4 ± 28.3% at 120 min. These findings suggest that both synaptic stimulation and membrane depolarization trigger dynamic and

sustained *Ube3a* upregulation, with depolarization eliciting a larger and earlier amplitude response.

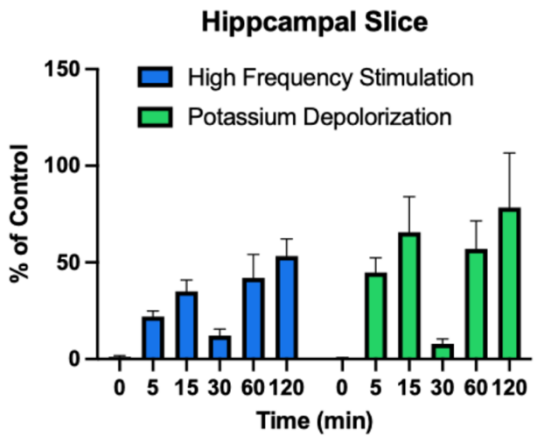

Figure 1. Time course of Ube3a protein induction in CA1 following neuronal activation. Western blot quantification of Ube3a levels in hippocampal CA1 slices following either high-frequency synaptic stimulation (5×100 Hz HFS at Schaffer collateral–CA1 synapse (n=7)) or potassium-induced depolarization (50 mM KCl) (n=7). Data are expressed as mean ± SEM percentage change from the unstimulated baseline (time 0, set to 0%). HFS elicited a rapid increase in Ube3a that peaked at ~35% by 15 min then rebounded to ~53% by 120 min. KCl depolarization produced a higher amplitude and earlier peak (~66% at 15 min), with a delayed maximum (~78%) at 120 min. Each time point represents n = 6 independent slice preparations. Data were analyzed using two-way repeated-measures ANOVA with "stimulus type" (HFS vs. KCl) and "time" (0, 5, 15, 30, 60, 120 min) as factors, followed by Bonferroni post hoc comparisons against the baseline (time 0) within each condition. Both main effects and the interaction were significant ($p < 0.001$). Under HFS, significant increases occurred at 5 min ($p = 0.003$), 15 min ($p = 0.001$), 60 min ($p = 0.02$), and 120 min ($p = 0.001$). Under KCl, significant elevation was observed as early as 5 min ($p = 0.001$), with maximum difference at 120 min ($p < 0.0001$). Normality (Shapiro–Wilk) and sphericity (Mauchly's test) assumptions were verified; Greenhouse–Geisser correction was applied when necessary.

The biphasic increases in Ube3a protein observed following both high-frequency stimulation and KCl-induced depolarization raise an important mechanistic consideration regarding the allelic origin of the observed changes. In wild-type hippocampal neurons, maternal Ube3a is the primary source of protein expression, as the paternal allele is subject to strong imprinting-mediated silencing. However, recent evidence indicates that the paternal allele is not absolutely silent but rather exhibits very low-level transcription and translation under basal conditions, with potential for context-dependent repression (Judson et al., 2014). In non-stimulated brain tissue from maternal *Ube3a* deficient, wild-type, and *Ube3a* knockout animals, that paternal expression can be detected in maternal Ube3a deficient tissues. However, it is unclear if the paternal-expressed protein detected in Figure 2 is derived from neuronal sources, or simply reflects other cells that exhibit biallelic expression, such as glial cells, astrocytes and oligodendrocytes.

The dynamic modulation of Ube3a protein following neuronal activity therefore raises the question of whether the biphasic response reflects activity-dependent regulation of maternal Ube3a alone, or whether transient alterations in paternal silencing contribute to the observed changes. The rapid early surge in protein abundance within minutes of stimulation is most consistent with activity-driven regulation of maternal protein stability and translation, yet the delayed secondary peak at 60–120 minutes may involve chromatin- or noncoding RNA–dependent mechanisms that partially relax paternal silencing. This is particularly relevant in the context of Angelman syndrome, where loss of maternal expression unmasks the therapeutic potential of harnessing even modest paternal *Ube3a* expression. Thus, these findings highlight the need to parse maternal- versus paternal-derived contributions to Ube3a dynamics in the hippocampus and other brain regions, as doing so will refine our understanding of activity-dependent plasticity and inform therapeutic strategies aimed at reactivating the silent allele. Disentangling the relative contributions of maternal and paternal *Ube3a* expression is technically challenging, as the two protein products are identical and thus indistinguishable in standard assays. Without selective disruption of one allele, which inherently perturbs the normal physiology of the wild-type brain, it remains difficult to determine whether activity-dependent changes in Ube3a arise solely from maternal regulation or from transient modulation of paternal silencing. This limitation underscores the need for allele-specific reporters or advanced epigenetic mapping strategies to resolve the dynamics of each allele in intact neuronal circuits. This challenge highlights the value of allele-specific reporter systems, such as the YFP-expressing Ube3a knock-in mouse model, which enables direct visualization and quantification of maternal versus paternal Ube3a contributions in vivo without perturbing overall protein function.

The Dindot laboratory developed a genetically engineered mouse model in which the endogenous *Ube3a* gene is modified to include an in-frame yellow fluorescent protein (YFP) tag at the C-terminus of the

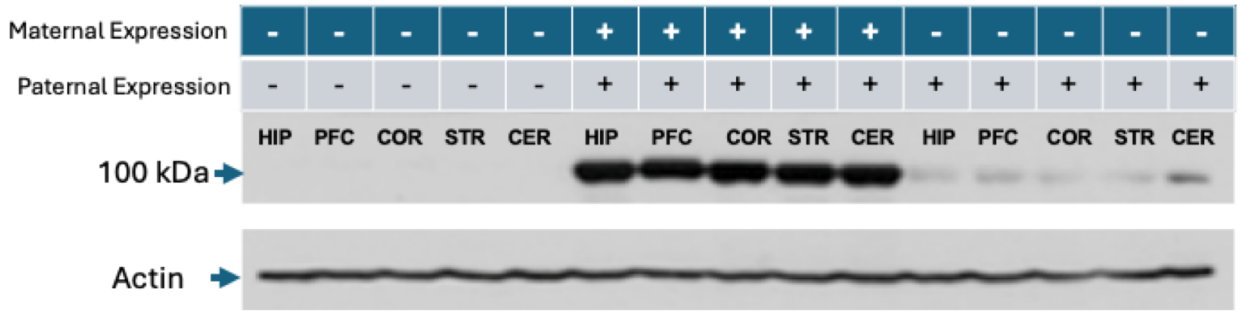

Figure 2. Regional Ube3a protein expression across genotypes. Western blot analysis of Ube3a protein levels in hippocampus (HIP), prefrontal cortex (PFC), cortex (COR), striatum (STR), and cerebellum (CER) from wild-type (+/+) mice, maternal *Ube3a* deletion (m−/p+) mice, and paternal *Ube3a* deletion (m+/p−) mice. As expected, maternal deletion resulted in a near-complete loss of Ube3a protein across all brain regions, while both maternal and paternal deletion animals showed no detectable Ube3a expression compared to wild-type, consistent with a majority, but not complete, paternal allele silencing. Actin (lower panel) served as a loading control.

Ube3a protein (Dindot et al., 2008). This modification enables direct visualization and biochemical discrimination of UBE3A protein isoforms derived from either the maternal or paternal allele. By using a breeding strategy in which the YFP-tagged allele is inherited either maternally or paternally, researchers can isolate the contribution of each parental allele to total *Ube3a* expression. This is of particular significance in the context of Angelman syndrome, where maternal *Ube3a* loss is pathogenic and paternal expression is normally silenced in neurons due to genomic imprinting. The model thus serves as a powerful genetic tool to dissect allele-specific expression dynamics under both basal and experimentally induced conditions.

The incorporation of the YFP tag increases the predicted molecular weight of the Ube3a protein by approximately 27 kilodaltons. YFP is a ~238–amino acid protein, and with an average amino acid molecular mass of ~110 Da, the added tag significantly shifts the migration of the protein in SDS–PAGE and Western blot analyses. This molecular weight shift enables simultaneous detection and discrimination between tagged and untagged alleles using a single Ube3a antibody, without the need for separate epitope-specific reagents. The mobility shift is especially advantageous when maternal and paternal alleles are differentially tagged in heterozygous mice, as it allows precise quantification of expression from each allele in the same lysate.

This YFP-tagged Ube3a model can be applied to studies of neuronal activation and synaptic plasticity by quantifying allele-specific Ube3a expression following defined stimuli. For example, after associative fear conditioning or other behaviorally relevant paradigms, brain regions can be harvested, and Western blot analyses can be performed to track changes in expression from the maternal versus paternal allele. Because the YFP tag does not interfere with Ube3a's E3 ubiquitin ligase function, and because both alleles can be independently visualized, the model provides a high-resolution approach for exploring the molecular and temporal dynamics of *Ube3a* regulation. This facilitates investigations into

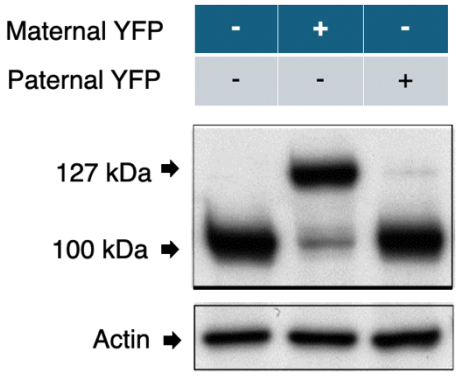

Figure 3. Allele-specific detection of Ube3a using a YFP-tagged *Ube3a* knock-in mouse model. Representative Western blot showing differential migration of YFP-tagged versus untagged Ube3a protein in brain lysates from mice inheriting the YFP-tagged *Ube3a* allele maternally (Mat-YFP), paternally (Pat-YFP), or both maternally and paternally (Mat+Pat-YFP). The addition of the YFP tag increases the apparent molecular weight of UBE3A by ~27 kDa, allowing clear separation of tagged and untagged forms on SDS–PAGE. In Mat-YFP animals, only the higher-molecular-weight YFP-tagged Ube3a band is detected, consistent with maternal allele-specific expression in neurons. In Pat-YFP animals, only the lower-molecular-weight untagged Ube3a band is present, reflecting paternal allele silencing in neurons. In Mat+Pat-YFP animals, both bands are visible, corresponding to the tagged maternal and untagged paternal alleles. β-actin was used as a loading control. This mobility shift enables direct biochemical discrimination of allele-specific Ube3a expression in the same sample.

mechanisms that may transiently unsilence the paternal allele or enhance maternal allele expression in response to neuronal activity, ultimately informing therapeutic strategies for Angelman syndrome that aim to modulate allele-specific expression.

Hippocampal Ube3a expression

Following associative fear conditioning, hippocampal lysates from *Ube3a-YFP* reporter mice revealed distinct temporal patterns of maternal and paternal Ube3a expression relative to no-shock controls (set to 0%). For maternal Ube3a, expression rose modestly at 1 min post-conditioning (18.99 ± 8.30%) before transiently declining at 5 min (4.20 ± 7.02%) and 15 min (−16.66 ± 7.35%). Levels remained reduced at 30 min (−12.18 ± 7.22%), but showed a marked increase by 1 hr (29.24 ± 6.59%), with further elevations at 3 hrs (35.67 ± 12.29%) and 6 hrs (49.60 ± 14.68%). Peak maternal expression occurred at 18 hrs post-conditioning, reaching 76.44 ± 13.47% above control values.

Paternal Ube3a expression followed a different trajectory. A rapid increase was observed at 1 min (23.78 ± 10.08%), followed by a transient suppression at 5 min (−1.01 ± 14.93%) and 15 min (−26.38 ± 2.91%). Expression began to rebound by 30 min (−8.94 ± 4.86%) and then surged dramatically at 1 hr (85.64 ± 15.82%), surpassing maternal levels at the same time point. This heightened paternal expression continued at 3 hrs (95.98 ± 14.05%) and peaked at 6 hrs (110.56 ± 19.65%), before declining to 54.63 ± 14.94% by 18 hrs. These data indicate that both maternal and paternal *Ube3a* are dynamically regulated in the hippocampus following associative fear conditioning, but with distinct timing and amplitude profiles, suggesting allele-specific contributions to experience-dependent protein regulation.

Prefrontal Cortex

Following associative fear conditioning, Ube3a-YFP protein levels in the prefrontal cortex were quantified separately for the maternal and paternal alleles using Western blotting. Data were normalized to the "no shock" control group, which was set to 0% change in expression. In the maternal allele, Ube3a levels showed a rapid and transient decrease immediately after training, with reductions observed at 1 min (−34.94 ± 9.07%) and 5 min (−21.15 ± 3.61%) post-conditioning. Expression began to recover by 15 min (−10.82 ± 16.25%) and showed a marked increase at 1 hr (69.42 ± 23.66%), peaking at 6 hrs (278.44 ±

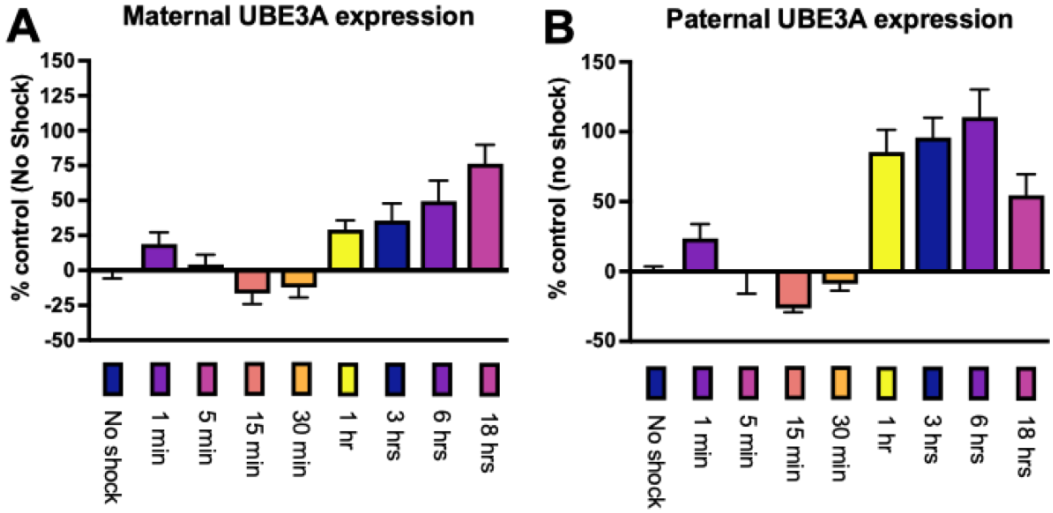

Figure 4. Temporal dynamics of maternal and paternal *Ube3a* expression in the hippocampus following associative fear conditioning in *Ube3a-YFP* reporter mice. Hippocampal lysates were collected from mice at the indicated time points after training and probed for YFP-tagged Ube3a via Western blot. Data are expressed as mean ± SEM percentage change from no-shock controls (set to 0%) (n=6). Maternal Ube3a (n=5) showed a modest increase at 1 min, transient suppression between 5-30 min, and a sustained rise from 1-18 hrs, peaking at 76.44% above baseline. Paternal Ube3a (n=5) exhibited a rapid increase at 1 min, a transient decrease at 5-15 min and a pronounced surge between 1-6 hrs, peaking at 110.56% above baseline before declining by 18 hrs. These data reveal distinct allele-specific temporal patterns of Ube3a regulation following fear conditioning.

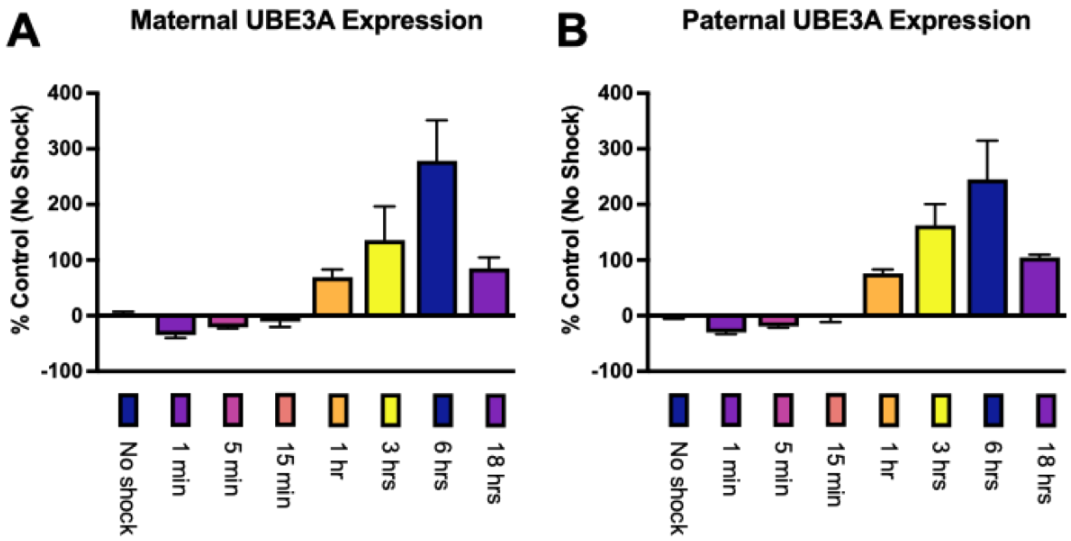

Figure 5. Time course of maternal and paternal Ube3a-YFP expression in the hippocampus following contextual fear conditioning. Western blot quantification of Ube3a-YFP levels was performed at 1 min, 5 min, 15 min, 1 hr, 3 hrs, 6 hrs, and 18 hrs post-conditioning in both maternal (left) and paternal (right) alleles. Data are expressed as mean ± SEM relative to the "no shock" control group (set to 0%)(n=6). Maternal allele expression (n=5) showed an initial decrease at early time points, followed by a robust increase peaking at 6 hrs. Paternal allele expression (n=5) exhibited a similar temporal pattern but with lower early repression and a slightly lower peak magnitude. Representative blots are shown above each graph. n values per group are indicated within the paternal dataset; maternal group sizes were matched.

126.69%). By 18 hrs, maternal expression had declined toward baseline (85.41 ± 33.72%), suggesting a time-limited post-training upregulation.

Paternal Ube3a expression followed a broadly similar temporal trajectory but with notable differences in amplitude and timing. Early post-conditioning time points showed modest decreases at 1 min (−30.01 ± 4.35%), 5 min (−19.45 ± 2.97%), and 15 min (−2.83 ± 12.05%). Expression then rose sharply at 1 hr (76.09 ± 12.11%), continued to increase at 3 hrs (162.56 ± 65.99%), and reached a peak at 6 hrs (245.11 ± 120.62%). Similar to the maternal allele, levels declined by 18 hrs (104.64 ± 7.49%). The parallel but distinct patterns between maternal and paternal expression suggest that both alleles contribute to the hippocampal Ube3a pool in an activity-dependent manner, with the maternal allele exhibiting slightly greater early repression and larger late-phase induction following fear conditioning.

Parietal Cortex

In the parietal cortex, maternal *Ube3a-YFP* expression demonstrated a rapid and robust increase following contextual fear conditioning. Compared to "no shock" controls, maternal allele expression rose sharply within 1 min (+169.1% ± 9.0%) and remained highly elevated at 5 min (+157.8% ± 15.1%) and 15 min (+123.0% ± 30.8%). Expression levels progressively declined thereafter, with moderate increases at 30 min (+80.9% ± 16.5%) and 1 hr (+18.8% ± 10.0%), before returning to baseline or slightly below control levels at 3 hrs (+14.5% ± 4.1%), 6 hrs (−21.2% ± 6.4%), and 18 hrs (−21.2% ± 6.4%). The early phase surge suggests a transient, time-locked maternal allele activation that diminishes within hours after conditioning.

Paternal allele expression followed a similar temporal profile, though with some differences in amplitude and decay kinetics. Paternal Ube3a-YFP levels rose to +160.9% ± 7.9% at 1 min and peaked at +171.9% ± 9.4% at 5 min. Expression remained moderately elevated at 15 min (+101.5% ± 38.2%) and 30 min (+96.9% ± 6.4%), before dropping substantially at 1 hr (+26.7% ± 10.5%) and 3 hrs (+10.9% ± 3.6%). By 6 hrs and 18 hrs, paternal expression decreased below baseline (−15.1% ± 3.5%). The parallel early activation of both maternal and paternal alleles suggests rapid transcriptional or post-translational modulation in the parietal cortex following learning, with a subsequent return to pre-conditioning levels within a short time window.

Discussion

Differences in Ube3a expression between hippocampus, parietal cortex, and prefrontal cortex following a learning paradigm are consistent with the

distinct yet interconnected roles these regions play within the cognitive and mnemonic network, and with the underlying neurobiology of Angelman syndrome (AS) models. Ube3a is a neuronally enriched E3 ubiquitin ligase that regulates proteostasis, synaptic plasticity, and experience-dependent structural remodeling of neuronal circuits (Greer et al., 2010). In the healthy brain, maternal Ube3a is robustly expressed in most forebrain neurons, while the paternal allele is epigenetically silenced through neuron-specific antisense transcription (Meng et al., 2012). In AS models, loss or manipulation of the maternal Ube3a allele unmasks region-specific vulnerabilities that reflect both the intrinsic molecular architecture of each region and its role within large-scale functional networks (Sato and Stryker, 2008; Wallace et al., 2012).

The hippocampus is a critical hub for encoding and consolidation of episodic and spatial memories, relying heavily on activity-dependent synaptic plasticity mechanisms, including long-term potentiation (Morris et al., 2003; Sweatt, 2004; Nabavi et al., 2014). Previous studies have shown that Ube3a is rapidly upregulated in hippocampal neurons following spatial learning, likely due to local translational control in dendrites and activity-triggered post-transcriptional modifications (Pastuzyn and Shepherd, 2017). This upregulation may support structural remodeling by degrading inhibitory synaptic proteins and modulating cytoskeletal regulators (Sun et al., 2015).

In AS models, the absence or altered dosage of maternal Ube3a may shift these region-specific dynamics in multiple ways. First, compensatory changes in synaptic protein turnover could be exaggerated in regions with higher plasticity demands, such as the hippocampus, producing more pronounced learning-induced changes than in associative cortical areas (Sato and Stryker, 2008). Second, the connectome-level role of Ube3a suggests that deficits in one hub region (e.g., hippocampus) can alter the pattern of activity and protein expression in downstream brain regions (e.g., parietal and prefrontal cortices), potentially amplifying or delaying the expression changes in those regions (Wallace et al., 2012). Finally, activity-dependent regulation of Ube3a itself is mediated, in part, through calcium-dependent

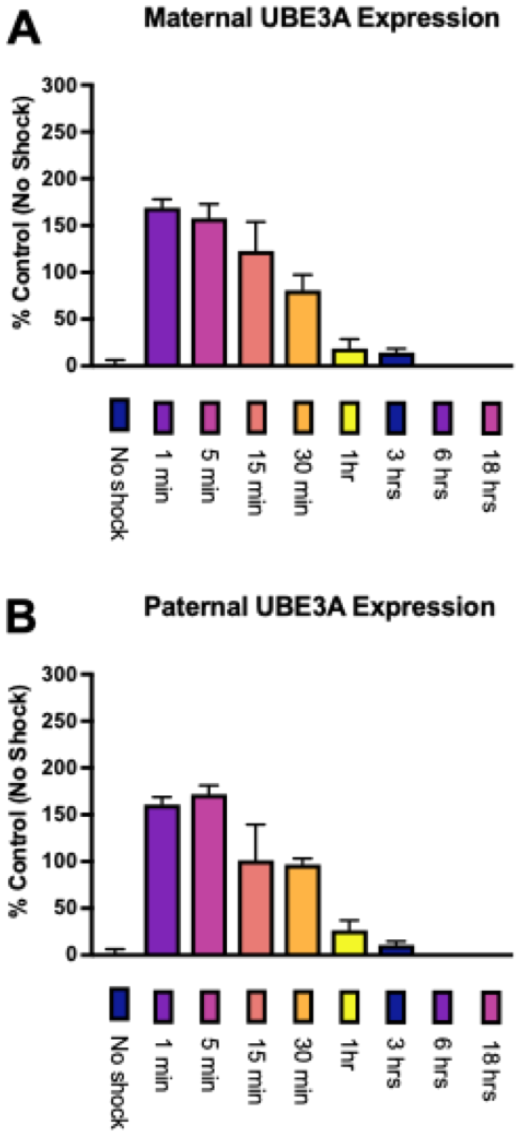

Figure 6. Time course of maternal and paternal *UBE3A-YFP* expression in the parietal cortex following contextual fear conditioning. Western blot quantification of Ube3a-YFP protein was performed at 1 min, 5 min, 15 min, 30 min, 1 hr, 3 hrs, 6 hrs, and 18 hrs post-conditioning. Data are expressed as mean ± SEM relative to the "no shock" control group (n=6) (set to 0%). Both maternal (n=5) and paternal alleles (n=5) showed rapid and large increases in expression within the first 5 min, followed by a gradual decline toward baseline, with levels falling below control values at later time points. Representative Western blots are shown above each graph. n values per group are indicated.

signaling cascades and translational control mechanisms (e.g., via mTOR), which may be differentially engaged across brain regions while learning a task or experiencing a substantial event (Huber et al., 2002; Hoeffer and Klann, 2010). Taken together, the observed region-specific changes are not

merely a reflection of anatomical location, but a functional manifestation of the distributed memory network's activity profile, the local plasticity rules, and the molecular pathology characteristic of AS.

Acknowledgements

This work was supported by Foundation for Angelman Syndrome Therapeutics, Grant Number: 6143108900.

References

Banko JL, Trotter J, Weeber EJ (2011) Insights into synaptic function from mouse models of human cognitive disorders. Future Neurol 6:113-125.

Buiting K, Williams C, Horsthemke B (2016) Angelman syndrome - insights into a rare neurogenetic disorder. Nat Rev Neurol 12:584-593.

Daily J, Smith AG, Weeber EJ (2012) Spatial and temporal silencing of the human maternal UBE3A gene. Eur J Paediatr Neurol 16:587-591.

Dindot SV, Antalffy BA, Bhattacharjee MB, Beaudet AL (2008) The Angelman syndrome ubiquitin ligase localizes to the synapse and nucleus, and maternal deficiency results in abnormal dendritic spine morphology. Hum Mol Genet 17:111-118.

Du X, Wei L, Yang B, Long S, Wang J, Sun A, Jiang Y, Qiao Z, Wang H, Wang Y (2023) Cortical and subcortical morphological alteration in Angelman syndrome. J Neurodev Disord 15:7.

Fang P, Lev-Lehman E, Tsai TF, Matsuura T, Benton CS, Sutcliffe JS, Christian SL, Kubota T, Halley DJ, Meijers-Heijboer H, Langlois S, Graham JM, Jr., Beuten J, Willems PJ, Ledbetter DH, Beaudet AL (1999) The spectrum of mutations in UBE3A causing Angelman syndrome. Hum Mol Genet 8:129-135.

Filonova I, Trotter JH, Banko JL, Weeber EJ (2014) Activity-dependent changes in MAPK activation in the Angelman Syndrome mouse model. Learn Mem 21:98-104.

Greer PL, Hanayama R, Bloodgood BL, Mardinly AR, Lipton DM, Flavell SW, Kim TK, Griffith EC, Waldon Z, Maehr R, Ploegh HL, Chowdhury S, Worley PF, Steen J, Greenberg ME (2010) The Angelman Syndrome protein Ube3A regulates synapse development by ubiquitinating arc. Cell 140:704-716.

Grier MD, Carson RP, Lagrange AH (2015) Toward a Broader View of Ube3a in a Mouse Model of Angelman Syndrome: Expression in Brain, Spinal Cord, Sciatic Nerve and Glial Cells. PLoS One 10:e0124649.

Gustin RM, Bichell TJ, Bubser M, Daily J, Filonova I, Mrelashvili D, Deutch AY, Colbran RJ, Weeber EJ, Haas KF (2010) Tissue-specific variation of Ube3a protein expression in rodents and in a mouse model of Angelman syndrome. Neurobiol Dis 39:283-291.

Hoeffer CA, Klann E (2010) mTOR signaling: at the crossroads of plasticity, moemory and disease. Trends Neurosci 33:67-75

Hsiao JS, Germain ND, Wilderman A, Stoddard C, Wojenski LA, Villafano GJ, Core L, Cotney J, Chamberlain SJ (2019) A bipartite boundary element restricts UBE3A imprinting to mature neurons. Proc Natl Acad Sci U S A 116:2181-2186.

Huber KM, Gallagher SM, Warren ST, Bear MF (2002) Altered synaptic plasticity in a mouse model of fragile X mental retardation. Proc Natl Acad Sci U S A 99:7746-7750.

Jiang YH, Armstrong D, Albrecht U, Atkins CM, Noebels JL, Eichele G, Sweatt JD, Beaudet AL (1998) Mutation of the Angelman ubiquitin ligase in mice causes increased cytoplasmic p53 and deficits of contextual learning and long-term potentiation. Neuron 21:799-811.

Jones KA, Han JE, DeBruyne JP, Philpot BD (2016) Persistent neuronal Ube3a expression in the suprachiasmatic nucleus of Angelman syndrome model mice. Sci Rep 6:28238.

Judson MC, Sosa-Pagan JO, Del Cid WA, Han JE, Philpot BD (2014) Allelic specificity of Ube3a expression in the mouse brain during postnatal development. J Comp Neurol 522:1874-1896.

Keute M, Miller MT, Krishnan ML, Sadhwani A, Chamberlain S, Thibert RL, Tan WH, Bird LM, Hipp JF (2021) Angelman syndrome genotypes manifest varying degrees of clinical severity and developmental impairment. Mol Psychiatry 26:3625-3633.

Malenka RC, Bear MF (2004) LTP and LTD: an embarrassment of riches. Neuron 44:5-21.

Martinez JL, Jr., Derrick BE (1996) Long term potentiation and learning. Annu Rev Psychol 47:173-203.

Meng L, Person RE, Beaudet AL (2012) Ube3a-

ATS is an atypical RNA polymerase II transcript that represses the paternal expression of Ube3a. Hum Mol Genet 21:3001-3012.

Meng L, Ward AJ, Chun S, Bennett CF, Beaudet AL, Rigo F (2015) Towards a therapy for Angelman syndrome by targeting a long non-coding RNA. Nature 518:409-412.

Morris RG, Moser EI, Riedel G, Martin SJ, Sandin J, Day M, O'Carroll C (2003) Elements of a neurobiological theory of the hippocampus: the role of activity-dependent synaptic plasticity in memory. Philos Trans R Soc Lond B Biol Sci 358:773-786.

Nabavi S, Fox R, Alfonso S, Aow J, Malinow R (2014) GluA1 trafficking and metabotropic NMDA: addressing results from other laboratories inconsistent with ours. Philos Trans R Soc Lond B Biol Sci 369:20130145.

Pastuzyn ED, Shepherd JD (2017) Activity Dependent Arc Expression and Homeostatic Synaptic Plasticity Are Altered in Neurons from a Mouse Model of Angelman Syndrome. Front Mol Neurosci 10:234.

Peters SU, Kaufmann WE, Bacino CA, Anderson AW, Adapa P, Chu Z, Yallampalli R, Traipe E, Hunter JV, Wilde EA (2011) Alterations in white matter pathways in Angelman syndrome. Dev Med Child Neurol 53:361-367.

Sato M, Stryker MP (2008) Distinctive features of adult ocular dominance plasticity. J Neurosci 28:10278-10286.

Selcher JC, Weeber EJ, Varga AW, Sweatt JD, Swank M (2002) Protein kinase signal transduction cascades in mammalian associative conditioning. Neuroscientist 8:122-131.

Sun S, Henriksen K, Karsdal MA, Byrjalsen I, Rittweger J, Armbrecht G, Belavy DL, Felsenberg D, Nedergaard AF (2015) Collagen Type III and VI Turnover in Response to Long-Term Immobilization. PLoS One 10:e0144525.

Sweatt JD (2004) Hippocampal function in cognition. Psychopharmacology (Berl) 174:99-110.

Thomas KL, Davis S, Hunt SP, Laroche S (1996) Alterations in the expression of specific glutamate receptor subunits following hippocampal LTP in vivo. Learn Mem 3:197-208.

Vihma H, Li K, Welton-Arndt A, Smith AL, Bettadapur KR, Gilmore RB, Gao E, Cotney JL, Huang HC, Collins JL, Chamberlain SJ, Lee HM, Aube J, Philpot BD (2024) Ube3a unsilencer for the potential treatment of Angelman syndrome. Nat Commun 15:5558.

Wallace ML, Burette AC, Weinberg RJ, Philpot BD (2012) Maternal loss of Ube3a produces an excitatory/inhibitory imbalance through neuron type-specific synaptic defects. Neuron 74:793-800.

Weeber EJ, Jiang YH, Elgersma Y, Varga AW, Carrasquillo Y, Brown SE, Christian JM, Mirnikjoo B, Silva A, Beaudet AL, Sweatt JD (2003) Derangements of hippocampal calcium/calmodulin-dependent protein kinase II in a mouse model for Angelman mental retardation syndrome. J Neurosci 23:2634-2644.

Yamasaki K, Joh K, Ohta T, Masuzaki H, Ishimaru T, Mukai T, Niikawa N, Ogawa M, Wagstaff J, Kishino T (2003) Neurons but not glial cells show reciprocal imprinting of sense and antisense transcripts of Ube3a. Hum Mol Genet 12:837-847.

Yoon HM, Jo Y, Shim WH, Lee JS, Ko TS, Koo JH, Yum MS (2020) Disrupted Functional and Structural Connectivity in Angelman Syndrome. AJNR Am J Neuroradiol 41:889-897.